

## MIT Open Access Articles

*Predicting vehicular emissions in high spatial resolution using pervasively measured transportation data and microscopic emissions model*

The MIT Faculty has made this article openly available. **Please share** how this access benefits you. Your story matters.

**Citation:** Nyhan, Marguerite et al. "Predicting Vehicular Emissions in High Spatial Resolution Using Pervasively Measured Transportation Data and Microscopic Emissions Model." Atmospheric Environment 140 (September 2016): 352–363 © 2016 Elsevier Ltd

**As Published:** <http://dx.doi.org/10.1016/J.ATMOENV.2016.06.018>

**Publisher:** Elsevier BV

**Persistent URL:** <http://hdl.handle.net/1721.1/118452>

**Version:** Author's final manuscript: final author's manuscript post peer review, without publisher's formatting or copy editing

**Terms of use:** Creative Commons Attribution-NonCommercial-NoDerivs License



1 **Predicting vehicular emissions in high spatial resolution using pervasively measured**  
2 **transportation data and microscopic emissions model**

3  
4 Marguerite Nyhan<sup>1,\*</sup>, Stanislav Sobolevsky<sup>2</sup>, Chaogui Kang<sup>3</sup>, Prudence Robinson<sup>1</sup>, Andrea  
5 Corti<sup>4</sup>, Michael Szell<sup>5</sup>, David Streets<sup>6</sup>, Zifeng Lu<sup>6</sup>, Rex Britter<sup>1</sup>, Steven R.H. Barrett<sup>7</sup>, Carlo  
6 Ratti<sup>1</sup>

7 <sup>1</sup>Massachusetts Institute of Technology, SENSEable City Laboratory, Cambridge, MA,  
8 United States.

9 <sup>2</sup>Centre for Urban Science and Progress, New York University, New York City, United States.

10 <sup>3</sup>Wuhan University, Wuhan, Hubei, China.

11 <sup>4</sup>Politecnico di Milano, 32 Piazza Leonardo da Vinci, Milano, Italy.

12 <sup>5</sup>Center for Complex Network Research, Department of Physics, Northeastern University,  
13 Boston, United States.

14 <sup>6</sup>Argonne National Laboratory, National Aeronautics and Space Administration (NASA),  
15 Lemont, Illinois, United States.

16 <sup>7</sup>Massachusetts Institute of Technology, Department of Aeronautics and Astronautics,  
17 Cambridge, MA, United States.

18 \*Corresponding author.

19

20

21 **Abstract**

22 Air pollution related to traffic emissions pose an especially significant problem in cities; this  
23 is due to its adverse impact on human health and well-being. Previous studies which have  
24 aimed to quantify emissions from the transportation sector have been limited by either  
25 simulated or coarsely resolved traffic volume data. Emissions inventories form the basis of  
26 urban pollution models, therefore in this study, Global Positioning System (GPS) trajectory  
27 data from a taxi fleet of over 15,000 vehicles were analyzed with the aim of predicting air  
28 pollution emissions for Singapore. This novel approach enabled the quantification of  
29 instantaneous drive cycle parameters in high spatio-temporal resolution, which provided the  
30 basis for a microscopic emissions model. Carbon dioxide (CO<sub>2</sub>), nitrogen oxides (NO<sub>x</sub>),  
31 volatile organic compounds (VOCs) and particulate matter (PM) emissions were thus  
32 estimated. Highly localized areas of elevated emissions levels were identified, with a spatio-  
33 temporal precision not possible with previously used methods for estimating emissions.  
34 Relatively higher emissions areas were mainly concentrated in a few districts that were the

35 Singapore Downtown Core area, to the north of the central urban region and to the east of it.  
36 Daily emissions quantified for the total motor vehicle population of Singapore were found to  
37 be comparable to another emissions dataset. Results demonstrated that high-resolution spatio-  
38 temporal vehicle traces detected using GPS in large taxi fleets could be used to infer highly  
39 localized areas of elevated acceleration and air pollution emissions in cities, and may become  
40 a complement to traditional emission estimates, especially in emerging cities and countries  
41 where reliable fine-grained urban air quality data is not easily available. This is the first study  
42 of its kind to investigate measured microscopic vehicle movement in tandem with  
43 microscopic emissions modeling for a substantial study domain.

44

45 **Keywords:** air quality, transportation, emissions, microscopic emissions model, microscopic  
46 vehicle movement.

47

## 48 1. Introduction

49

50

51 With mass urbanization happening at an unprecedented scale, urban air quality is becoming  
52 an issue of global concern (WHO, 2014). Growth in populations, traffic, industrialization and  
53 energy usage have led to increased air pollution levels and subsequent public health effects at  
54 the urban, regional and global scale (Akimoto, 2003; Molina et al., 2004; Gurhar et al., 2010)  
55 The World Health Organization estimates that ambient air pollution leads to approximately  
56 3.7 million premature deaths annually worldwide, with South-East Asia and the Western  
57 Pacific Regions having the largest air pollution-related health burden (WHO, 2014).

58

59 The adverse impact of air pollution exposure on human health is well documented in the  
60 literature (WHO, 2014). Epidemiological studies have quantified the relationship between  
61 adverse health effects and both long- and short-term exposure to air pollution (Bell et al.,  
62 2004; Jerrett et al., 2005; Laden et al., 2006; Lewtas, 2007; Krewski et al., 2009; Nyhan et al.,  
63 2014a; Nyhan et al., 2014b). In assessing the impact of air pollution on mortality in the  
64 United States, Caiazzo et al. (2013) reported that the largest sector contributor of pollutant-  
65 related mortalities is road transportation, causing approximately 53,000 PM<sub>2.5</sub>-related deaths  
66 and approximately 5000 ozone-related deaths per year. These figures corresponded to  
67 premature deaths from cardiovascular diseases and lung cancer due to long-term exposure to  
68 PM<sub>2.5</sub> (where PM<sub>2.5</sub> refers to the particulate matter fraction which is less than 2.5µm in  
69 aerodynamic diameter).

70

71 Traditional methods for monitoring urban air quality employ discrete measurement stations  
72 which sample atmospheric conditions at specific sites throughout a city. Networks vary both  
73 in size and scale. The London Air Quality Network has over 50 sites classified as roadside,  
74 background, suburban and industrial that are dispersed throughout the whole metropolitan  
75 area (Laxen et al., 2003). Singapore, which is the focus of this study, has 14 high-grade  
76 stations operated by the National Environment Agency, gathering data throughout the island  
77 (NEA, 2015). Traditional approaches to monitoring air quality have several limitations,  
78 including significant investment required to set up and maintain the measurement networks.  
79 Furthermore, as air quality can exhibit large variations over a relatively small scales (Britter  
80 and Hanna, 2003), sampling biases can be introduced which make the assessment of human  
81 exposure and the sources of pollutants difficult (Vardoukalis et al., 2005). As a result of this,

82 municipal air quality monitoring is often supplemented by air quality models such as the  
83 AERMOD modeling system (USEPA, 2009) and the ADMS Urban model (CERC, 2015) to  
84 improve the spatial and temporal resolution of air pollution estimates. Sparsely located air  
85 quality monitors are limited in their usefulness for accurately determining the locations of air  
86 pollution sources. Therefore, air quality monitoring using distributed networks of sensors has  
87 gained traction as sensors are becoming smaller, less expensive yet more reliable (Chong et  
88 al., 2003; Burke et al., 2006; Cuff et al., 2008; Paulos et al., 2009; Kumar et al., 2015),  
89 providing a wealth of high spatial resolution air quality information.

90  
91 The availability of large transportation and mobility datasets from sensors, Global Positioning  
92 System (GPS)-enabled devices, along with improvements in methods and computational  
93 facilities for analyzing these have led to advancements in the field of urban computing  
94 research in recent times. So-called opportunistic sensing which is the use of data that is  
95 collected for one purpose but can be reused for another one (Campbell et al., 2008), has  
96 proved useful in many research studies. Examples include using various anonymized or  
97 aggregated spatio-temporal datasets created by different aspects of human activity, such as  
98 cell phone data (Gonzales et al, 2008; Sobolevsky et al, 2013; Hoteit et al, 2014; Kung et al,  
99 2014; Pei et al, 2014; Grauwin et al, 2014) or vehicle GPS traces (Kang et al, 2013). One  
100 such example of opportunistically utilizing vehicle GPS traces is a recent study by Santi et  
101 al., (2014) where the economic and environmental benefits of vehicle pooling in New York  
102 were quantified based on the analyses of a taxi GPS dataset consisting of 150 million trips.

103  
104 Emissions from on-road motor vehicles constitute one of the largest contributions to air  
105 pollutants such as carbon monoxide, nitrogen dioxide, ozone, selected volatile organic  
106 compounds and fine particulates (Molina and Molina, 2004), and also represent a factor in the  
107 spatial variability of air quality in urban areas (Fecht et al., 2016). Vehicle emissions have  
108 typically been estimated with the use of either measured (through loop detectors or similar) or  
109 modeled (using a transport simulator) traffic data. Based on this information, emission factors  
110 are commonly used to convert traffic loads into emissions (NARSTO, 2005). Emission  
111 factors vary from location to location, and depend on the vehicle model and road conditions  
112 (Zhang and Morawska, 2002; North et al., 2006). The application of emission factors to  
113 traffic loads is unable to account for real driving conditions as they happen on the road  
114 (Samuel et al., 2002). Thus, as an alternative, different vehicles models with different load  
115 factors are often used as probes, whose emissions (and eventually the emission of nearby

116 vehicles) are measured on the road (Canagaranta et al., 2004; Shorter et al., 2005). The  
117 aforementioned approaches do not allow the high resolution spatiotemporal mapping of  
118 emissions as they do not take into account the 'drive cycle' which is the description of a  
119 vehicle's velocity over time. The drive cycle allows the precise determination of consumption  
120 and hence emissions (Mantazeri et al., 2003; Int Panis et al., 2006). In the widely used  
121 MOBILE Model (USEPA, 2012), only 14 different drive cycles are used; however, these are  
122 only expressed as average speed. Many studies have examined the impact of different vehicle  
123 modes (idling, moving and accelerating) on the release of pollutants. In a study by Frey et al.,  
124 (2003) average emissions were observed to be five times greater during periods of  
125 acceleration for hydrocarbons and carbon dioxide, and reached ten times as much for nitric  
126 oxide and carbon monoxide compared with levels found in an idling vehicle. Similarly,  
127 ultrafine particulates released whilst a vehicle is accelerating have also been shown to  
128 increase significantly (Fruin et al., 2008). Hence, there is a need for the use of more detailed  
129 drive cycles, including velocity and acceleration parameters resolved in high spatial and  
130 temporal resolution, in modeling emissions from transportation.

131  
132 Many studies have led to the development of models that consider variations in speed and are  
133 appropriate for instantaneous emission modeling. These include the Comprehensive Modal  
134 Emissions Model developed at the University of California (An et al., 1997; Barth et al.,  
135 2006) and others (e.g. Rakha et al., 2004; Pelkmans et al., 2004; El-Sgawarby et al., 2005).  
136 Along with this, significant effort has been devoted to the use of micro-simulation methods  
137 for transportation modeling on road networks, for representing real-time, behavior-based  
138 policies (e.g. Ben-Akiva et al., 1997; Hu and Mahmassani, 1997; Liu et al., 2006). Individual  
139 driver behavior and individual vehicle's real-time space-time trajectories are explicitly  
140 represented through traffic micro-simulation models and these produce detailed vehicle  
141 operation, instantaneous speed and acceleration of vehicles that are necessary for microscopic  
142 emissions models. A review by Fontes et al., (2015) examined combining various micro-  
143 simulation tools for assessing the impacts of road traffic on the environment, and identified  
144 best practices which would aim to minimize errors in combining these. Int Panis et al., (2006)  
145 presented a methodology for making instantaneous emission modeling compatible with  
146 traffic micro-simulation models. In particular, the emissions caused by acceleration and  
147 deceleration of vehicles were modeled based on microscopic traffic simulation model  
148 integrated with an instantaneous emission model. The functions developed by Int Panis et al.,  
149 (2006) were incorporated into a study addressing optimum mitigation strategies for urban

150 transportation emissions by Osorio and Nanduri (2015) where a combination of macroscopic  
151 and microscopic traffic simulators and emissions models were employed.

152

153 Recent developments in the field of vehicle emissions have seen the uptake of cell phones  
154 and their built in sensors as on-board diagnostic systems - using the data gathered from the  
155 GPS and accelerometer to monitor the drive cycle and hence consumption and emissions  
156 (Thiagarajan et al., 2009). These approaches have been mostly confined to single or small  
157 numbers of vehicles. In this study, however, it is intended to extend an emissions model to a  
158 large vehicle fleet using GPS data collected. Intelligent Speed Adaption (ISA) systems are  
159 technologies which incorporate GPS navigation to apply speed limits to cars on specific road  
160 areas. Systems for monitoring and controlling vehicle velocities include ISA systems  
161 (Duynstee et al., 2001; Int Panis et al., 2006). These could also be used for reducing  
162 emissions and fuel consumption on road networks, but require fine-grained emissions  
163 predictions based on real-time GPS data.

164

165 The purpose of this study is to use data routinely captured by existing transportation networks  
166 and vehicle fleets to predict vehicular emissions in high spatial resolution. For this, GPS  
167 measurements gathered by a large taxi fleet in Singapore would be analyzed. Parameters  
168 representative of vehicle drive cycles would then be characterized in high spatial and  
169 temporal resolution at points throughout the road network. A microscopic emissions model  
170 would be implemented to predict the emissions of carbon dioxide (CO<sub>2</sub>), nitrogen oxide  
171 (NO<sub>x</sub>), volatile organic compounds (VOCs) and particulate matter (PM) throughout the study  
172 domain, where particulate matter here refers to total suspended particles. Highly localized  
173 areas of elevated emissions would thereby be identified, with a higher spatiotemporal  
174 precision than commonly used methods. This is the first study to implement a microscopic  
175 emissions model using measured microscopic vehicle trajectory data for an entire urban  
176 region.

177

## 178 **2. Methodology**

179

180

### 181 **2.1. Overview of methodology**

182

183 In order to develop an emissions inventory, GPS trajectory data from 15,236 taxis were  
184 analyzed. From this, the instantaneous parameters of velocity and acceleration were derived  
185 and used as inputs for a microscopic emissions model. Emissions of CO<sub>2</sub>, NO<sub>x</sub>, VOCs and  
186 PM were predicted across the road network of Singapore using this model. An analyses was  
187 completed which compares the taxi data used to the overall traffic on the road network in  
188 Singapore. Following this, emissions from the remainder of the total motor vehicle  
189 population of Singapore were also estimated. The results were compared to emissions  
190 estimates produced to those attained from the National Aeronautical and Space Agency  
191 (Streets and Lu, 2012).

192

193

### 194 **2.2. Study domain and GPS data processing**

195

196 The study domain included the island of Singapore, which covers approximately 718 km<sup>2</sup>.  
197 Singapore has a population of 5,469,700 people (Singapore Department of Statistics, 2014),  
198 therefore has an average population density of 7,618 persons per km<sup>2</sup>.

199

200 Our analysis used vehicle GPS traces collected over a period of one week from 15,236 taxis  
201 in Singapore. The raw data included the following parameters: identification number of the  
202 vehicle, a timestamp of when each location measurement was performed, the corresponding  
203 latitude and longitude defining the position of the vehicle. The data samples were collected at  
204 varying temporal intervals every few seconds. Our data was collected from an undisclosed  
205 vehicle fleet operator, which operates over the majority of the island of Singapore on a 24-  
206 hour basis. Each vehicle contained within the fleet transmits information including its  
207 identification number, location and status at various intervals to a central operations base. The  
208 dataset contained over 120 million vehicle-GPS samples measured from the 21<sup>st</sup> February  
209 2011 to the 27<sup>th</sup> February 2011.

210



211 The GPS trace data was utilized to infer both the location of each vehicle, its velocity and its  
212 acceleration. In applying a data cleaning process to the dataset, erroneous GPS points which  
213 fell outside the boundary of Singapore or which have an unreasonable distance from its  
214 previous location at a given time interval ( $\text{distance/time} \leq 150 \text{ km/h}$ ) were eliminated. The  
215 instantaneous velocities of vehicles were determined based on the time and distance between  
216 geo-referenced points. The data was filtered so as to only examine changes in velocity that  
217 occurred over short temporal ranges, where two consecutive data points were separated by no  
218 more than 5 seconds as intervals greater than this are unable to depict the microstructure of  
219 the acceleration profile. A secondary filtering process was applied to the data to remove  
220 errors attributed to GPS measurements, as these may be affected by the multi-path effect  
221 within urban canyons (Parkinson, 1996). An outlier filter was used that removed all the  
222 acceleration values that exceeded  $10 \text{ ms}^{-2}$  as these values are generally not attainable in an  
223 average car. The normative driving cycle, used to homologate vehicles emissions are  
224 characterized by a maximum acceleration of  $1.5 \text{ ms}^{-2}$  for FTP-72 and  $4 \text{ ms}^{-2}$  for LA92  
225 (Guzella and Sciarreta, 2005; Metric Mind Corporation, 2012), therefore sampling points  
226 with an acceleration value between  $0.5$  and  $10 \text{ m s}^{-2}$  were used in this study.

227

228

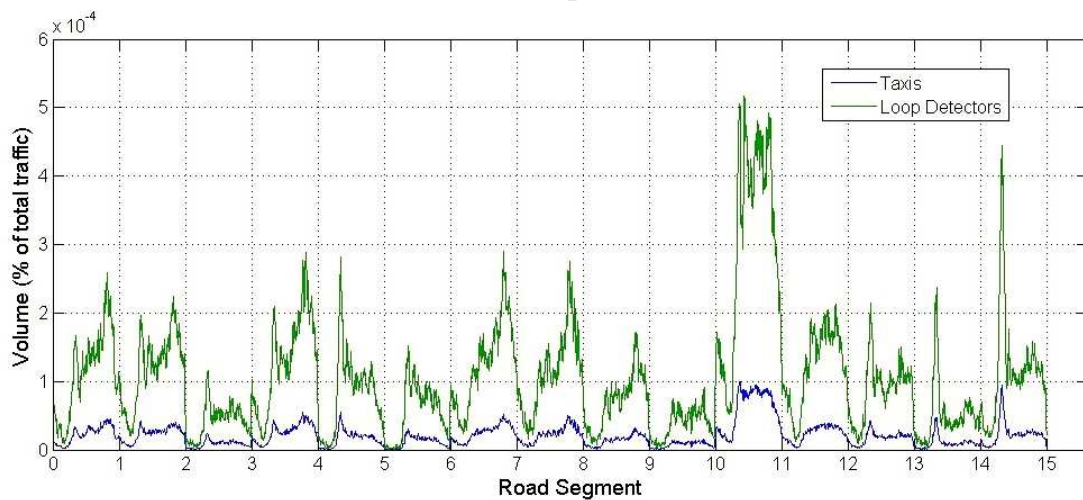
### 229 ***2.3. Comparison of taxi fleet and total traffic***

230 By applying the above filters, the distribution of the sampling intervals of the 15,236 taxis,  
231 indicate that only 7.71% of the logged data has a sampling interval of less than 5 seconds as  
232 well as a valid acceleration value. This indicates that the majority of vehicles demonstrate  
233 intermittent data logging at intervals greater than 5s. The spatial distribution of the valid  
234 samples was correlated with a co-efficient of determination of 0.75 to the spatial distribution  
235 of the raw vehicle-GPS points. In order to examine the spatial distributions of GPS points, the  
236 city was divided into road links. The valid accelerations of all the vehicles were then  
237 attributed to one of the road links based on their latitude and longitude data, and were  
238 projected onto a map of Singapore.

239

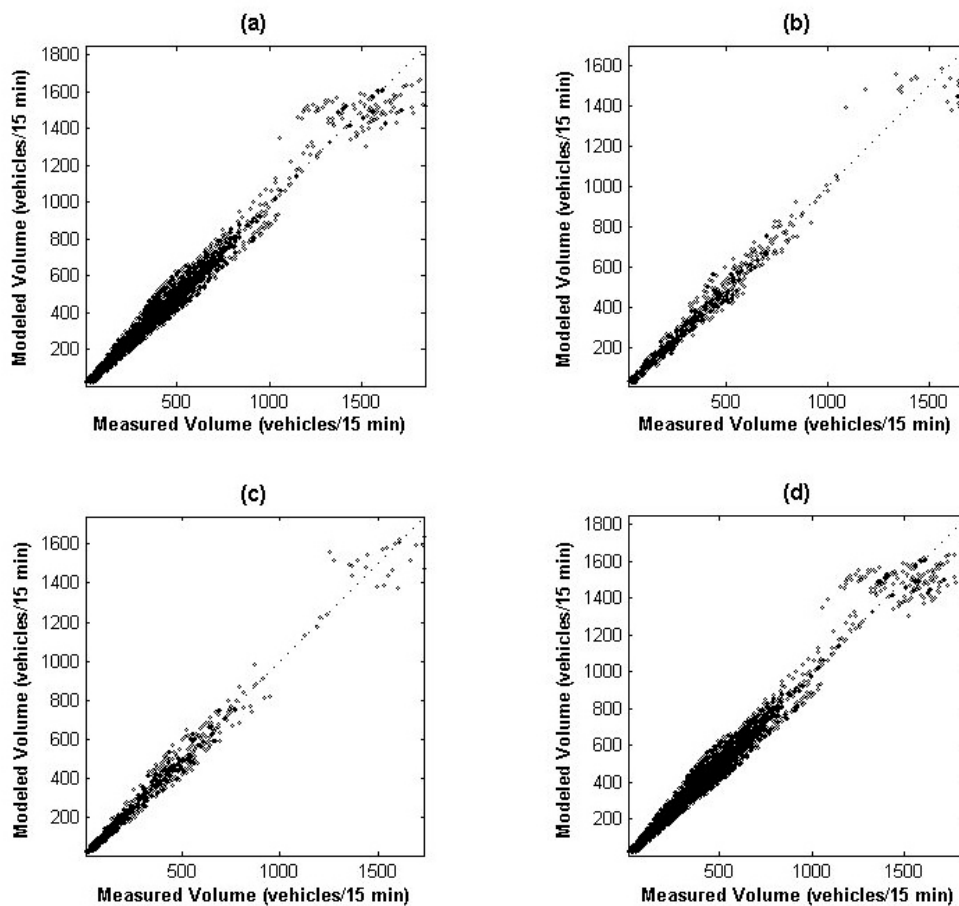
240 Aslam et al., (2012) demonstrated that vehicular GPS taxi network data can be used to infer  
241 general traffic patterns in Singapore. Aslam et al., (2012) used data from the same taxi fleet as  
242 used herein this study. Measured traffic data (i.e. counts of vehicles on road links per time  
243 intervals) were obtained through loop count data from the Land Transport Authority (LTA) of  
244 Singapore. By examining the fraction of road segments the taxi fleet covers during workdays,

245 it was concluded that 700 taxis were sufficient to cover 70% of the roads for the majority of  
 246 the day's 1-hour time windows, with the exception of those in the middle of the night when  
 247 vehicle numbers are sparse. Further to this, Aslam et al., (2012) also observed that 2000 taxis  
 248 were sufficient to cover 90% of the total loop detector locations during a period of 15 minutes  
 249 in the morning (from 08:00~08:15) on all workdays. Similarly, we compared our taxi fleet  
 250 data to measured traffic data obtained from loop detectors operated by Singapore's LTA for  
 251 the same time period as our study. To achieve this, the taxi data was synchronized with the  
 252 loop detector data, which was aggregated every 15 minutes. The time series of GPS points for  
 253 taxis were first matched to road links and then segments on the road network of Singapore.  
 254 The number of taxis on road segments where loop detectors are located, were counted every  
 255 15 minutes. These counts were then compared to the loop counts which were regarded as the  
 256 ground truth for traffic conditions. Figure 1 shows the taxi and loop detector count data for 15  
 257 randomly selected Singapore road segments. The taxi distribution tended to underestimate the  
 258 loop distribution and this underestimation was variable across road segments. On each road  
 259 link, a bias was observed which varied throughout the day, however this bias was relatively  
 260 consistent across days.  
 261



262  
 263 **Figure 1.** Distribution of traffic volumes (i.e. number of vehicles per road segment) on 15  
 264 randomly selected road segments for the 23rd February 2011. The x-axis includes 15 road  
 265 segments including a point for every 15 minutes during the 24-hour day. The y-axis  
 266 represents the percentage of traffic at that location and time. The taxi distribution (in blue)  
 267 underestimates the loop distribution (in green) and the underestimation is variable.  
 268

269 For inferring general traffic patterns, an artificial neural network model was employed, as has  
 270 been used in another study for predicting traffic volumes on road links (Moretti et al., 2015).  
 271 The model utilized was a simple corrective model for inferring vehicle distribution as  
 272 detected by loop detectors from vehicle distribution as determined by the taxi fleet. A 2-layer  
 273 feed-forward network was implemented, with a tan-sigmoid transfer function in the hidden  
 274 layer and linear transfer function in the output layer. The model was run for 500 road  
 275 segments. In determining the performance of the model, a linear regression between modeled  
 276 traffic volume and the corresponding targets of measured traffic volume was conducted.  
 277 Figure 2 shows the results of learning for trained model for a sample of data points. As there  
 278 is a strong association between the modeled and measured traffic volumes, this demonstrates  
 279 that the taxi fleet data may be used to predict general traffic on specific road segments, and  
 280 the results were similar across the road network of Singapore.  
 281



282  
 283 **Figure 2.** Results of the feed-forward artificial neural network model implementation.  
 284 Regression plot of a partial set of modeled traffic volumes versus corresponding measured  
 285 traffic volume for the (a) training phase ( $R^2=96\%$ ), (b) validation phase ( $R^2=93\%$ ), (c) testing

286 phase ( $R^2=92\%$ ) and (d) overall model ( $R^2=94\%$ ). A sub-sample of points are presented for  
 287 clarity.

288

#### 289 **2.4. Microscopic emissions model**

290

291 A microscopic emissions model was implemented and this computed the instantaneous air  
 292 pollution emissions associated with  $\text{CO}_2$ ,  $\text{NO}_x$ , VOCs and PM. The emissions model was  
 293 based on a model developed by Int Panis et al., (2006), and has been adopted by Osorio and  
 294 Nanduri (2015). The model utilizes instantaneous velocity and accelerations derived from the  
 295 GPS dataset to compute emissions. The emission rate at a given time-instant  $t$  is given in the  
 296 following equation:

$$297 \quad ER_n^k(t) = \max[E_{0n}^k, f_{1n_1}^k + f_{2n}^k v_n(t) + f_{3n}^k v_n(t)^2 + f_{4n}^k a_n(t) + f_{5n}^k a_n(t)^2 + f_{6n}^k v_n(t) a_n(t)], \quad (1)$$

298 where  $k$  is the pollutant type, i.e.  $k \in \{\text{CO}_2, \text{NO}_x, \text{VOC}, \text{PM}\}$ ,  $v_n(t)$  is the instantaneous  
 299 speed of vehicle  $n$  at time  $t$  (in m/s),  $ER_n^k(t)$  is the instantaneous emissions rate of pollutant  
 300  $k$  (in g/s),  $a_n(t)$  is the instantaneous acceleration of vehicle  $n$  at time  $t$  (in  $\text{m/s}^2$ ),  $E_{0n}^k$  is the  
 301 lower limit of emission rate for each pollutant type (in g/s), and  $f_{1n}^k, f_{2n}^k, f_{3n}^k, f_{4n}^k, f_{5n}^k$  and  
 302  $f_{6n}^k$  are the emission rate constants specific to each vehicle and pollutant type. Equation (1)  
 303 holds for  $\text{CO}_2$  and PM emissions. For  $\text{NO}_x$  and VOC emissions, the emissions rate  
 304 coefficients differ depending on whether the vehicle is in acceleration or deceleration mode.  
 305 If  $a_n(t) \geq -0.5 \text{ m/s}$ , then

$$306 \quad ER_n^k(t) = \max[E_{0n}^k, f_{1n_1}^k + f_{2n}^k v_n(t) + f_{3n}^k v_n(t)^2 + f_{4(1)n}^k a_n(t) + f_{5(1)n}^k a_n(t)^2 + f_{6(1)n}^k v_n(t) a_n(t)], \quad (2)$$

307 Otherwise, if  $a_n(t) < -0.5 \text{ m/s}$ , then

$$308 \quad ER_n^k(t) = \max[E_{0n}^k, f_{1n_1}^k + f_{2n}^k v_n(t) + f_{3n}^k v_n(t)^2 + f_{4(2)n}^k a_n(t) + f_{5(2)n}^k a_n(t)^2 + f_{6(2)n}^k v_n(t) a_n(t)], \quad (3)$$

309 The lower limit of the emissions rate  $E_0$  is fixed to zero for all pollutant types and vehicle  
 310 types. The emission rate constants (e.g.,  $f_1, f_2$ , etc.) are specified for each pollutant type and  
 311 vehicle type, and were determined from emissions measurements of on-road instrumented  
 312 vehicles. These were determined for the car, heavy duty vehicle (HDV, diesel) and bus  
 313 (diesel) categories. A table describing these emission rate constants are described in Int Panis  
 314 et al., (2006).

315 For each pollutant, the expected total emissions (in g) in the specified vehicle network during  
 316 the simulation period were computed by:

$$317 \quad E[TE^k] = \sum_{l \in L} E[TE_l^k], \quad (4)$$

318 where  $L$  is the set of all road links in the network, and  $E[TE_l^k]$  denotes the total emissions (in  
 319 g) of pollutant  $k$  on link  $l$ . The latter term in Equation (4) is approximated by:

$$320 \quad E[TE_l^k] = E[ER^{k,l}]E[T_l]\lambda_l\Delta T, \quad (5)$$

321 where  $E[ER^{k,l}]$  denotes the expected emissions rate (in g/s) for link  $l$  and pollutant type  $k$ ,  
 322  $E[T_l]$  is the travel time on link  $l$ ,  $\lambda_l$  is the arrival rate of vehicles to link  $l$  and  $\Delta T$  is the total  
 323 simulation time. For a given link  $l$  and pollutant type  $k$ , the term  $\lambda_l\Delta T$  approximated the  
 324 expected total demand over the time period of interest, while  $E[ER^{k,l}]E[T_l]$  approximated the  
 325 expected emissions per vehicle. The emissions computed for each road link were projected  
 326 onto a map of Singapore.

327

328 Emissions for the total motor vehicle population, represented by general traffic patterns,  
 329 across the road network of Singapore were quantified. Emissions were estimated on a daily  
 330 basis according to Equation (5). In this scenario however, the arrival rates of vehicles to each  
 331 road link,  $\lambda_l$ , were predicted using the traffic model described in Section 2.3. Daily emissions  
 332 were calculated for each of five days of data available, and the mean of these five days was  
 333 then compared to mean daily emissions estimated by Streets and Lu, (2012).

334

### 335 **2.5. Vehicle fleet composition**

336

337 The emissions model took into consideration the estimated composition of the vehicle fleet of  
 338 Singapore. This was based on information collected by the Land Transport Authority of  
 339 Singapore (LTA, 2015). The data-set yielded counts of the various categories of motor  
 340 vehicles within the overall transportation fleet i.e. Cars, Taxis, Motorcycles, Goods and Other  
 341 Vehicles, and Buses, and these categories were further stratified by type of fuel used i.e.  
 342 petrol, diesel, petrol-electric, petrol-CNG, CNG and electric for each of the respective  
 343 categories of vehicle type. Data for the year 2011 were used as this corresponded to our  
 344 vehicle data-set (see Table 1 for details).

345

346 **Table 1.** Motor vehicle population in Singapore by category and type of fuel used for the year  
 347 2011. Figures exclude tax exempted vehicles for off-the-road use (RU plates).

<b>Cars</b>	Petrol	596,947
	Diesel	346
	Petrol-Electric	3,786
	Petrol-CNG	2,642
	CNG	-
	Electric	2
	Total	603,723
<b>Taxis</b>	Petrol	279
	Diesel	23,880
	Petrol-Electric	56
	Petrol-CNG	2,836
	CNG	-
	Electric	-
Total	27,051	
<b>Motorcycles</b>	Petrol	145,672
	Electric	8
	Total	145,680
<b>Goods &amp; Other Vehicles</b>	Petrol	9,058
	Diesel	136,076
	Petrol-Electric	1
	Petrol-CNG	14
	CNG	8
	Electric	1
	Diesel-Electric	-
Total	145,158	
<b>Buses</b>	Petrol	194
	Diesel	16,433
	Petrol-Electric	-
	Petrol-CNG	8
	CNG	14
	Electric	3
Total	16,652	

348

### 349 3. Results

350

351

#### 352 *3.1. Spatial distribution of accelerations and predicted emissions*

353

354 Figure 3 shows counts of all valid acceleration data on each link on the road network. Higher  
355 counts of valid accelerations were concentrated in the Singapore Downtown Core area, at  
356 Changi International Airport and some parts of Jurong, Bishan and Yishun. As demonstrated  
357 in Section 3.3., the taxi data may be used to predict general traffic on road segments,  
358 therefore counts of valid accelerations were proportional to the distribution of vehicles in the  
359 city, and proportional to the number of accelerations of each road link. Valid accelerations on  
360 each road link were utilized for the emissions model. However, areas such as the Singapore  
361 Downtown Core area and the vicinity of Changi International Airport which were  
362 characterized by a relatively higher number of sample points of acceleration than other areas.  
363 This may indicate a bias in the dataset.

364

365 The spatial distributions of vehicle emissions computed for each road link in Singapore are  
366 shown in Figure 4. With regards emissions related to specific parameters, we can see that for  
367 all of CO<sub>2</sub>, NO<sub>x</sub>, VOC and PM, elevated levels were identified in a concentrated number of  
368 locations in the Singapore Downtown Core area, south of Newton and in Geylang. Elevated  
369 levels were also identified in the area surrounding Changi International Airport, Bishan and  
370 Jurong West.

371

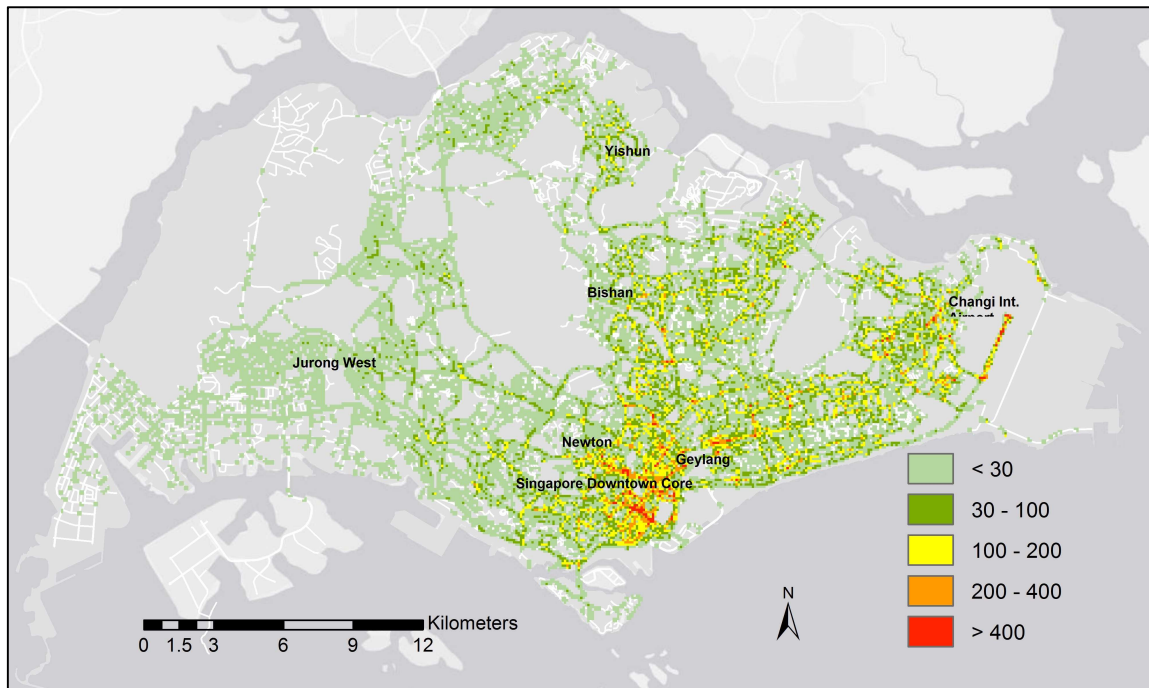
372

373

374

375





376

377 **Figure 3.** Spatial distribution of the number of valid accelerations in Singapore on the 23<sup>rd</sup>

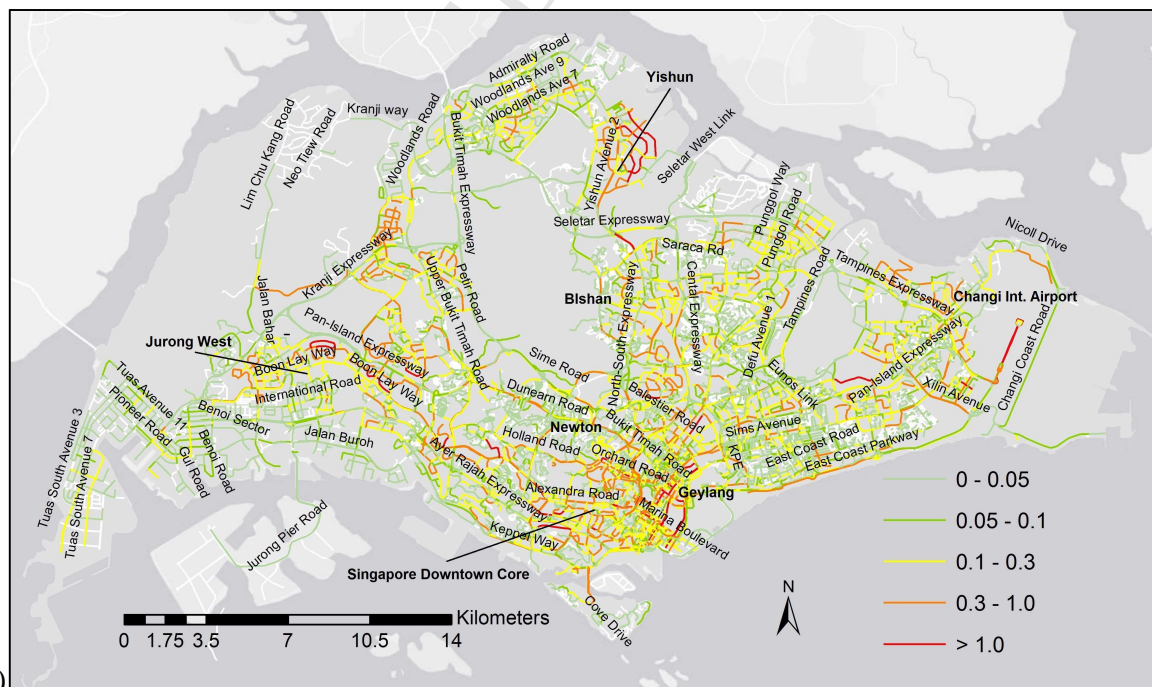
378 February 2011. Locations where relatively higher numbers of valid accelerations are

379 observed in the vicinity of the Singapore Downtown Core area and the Changi International

380 Airport in the east.

381

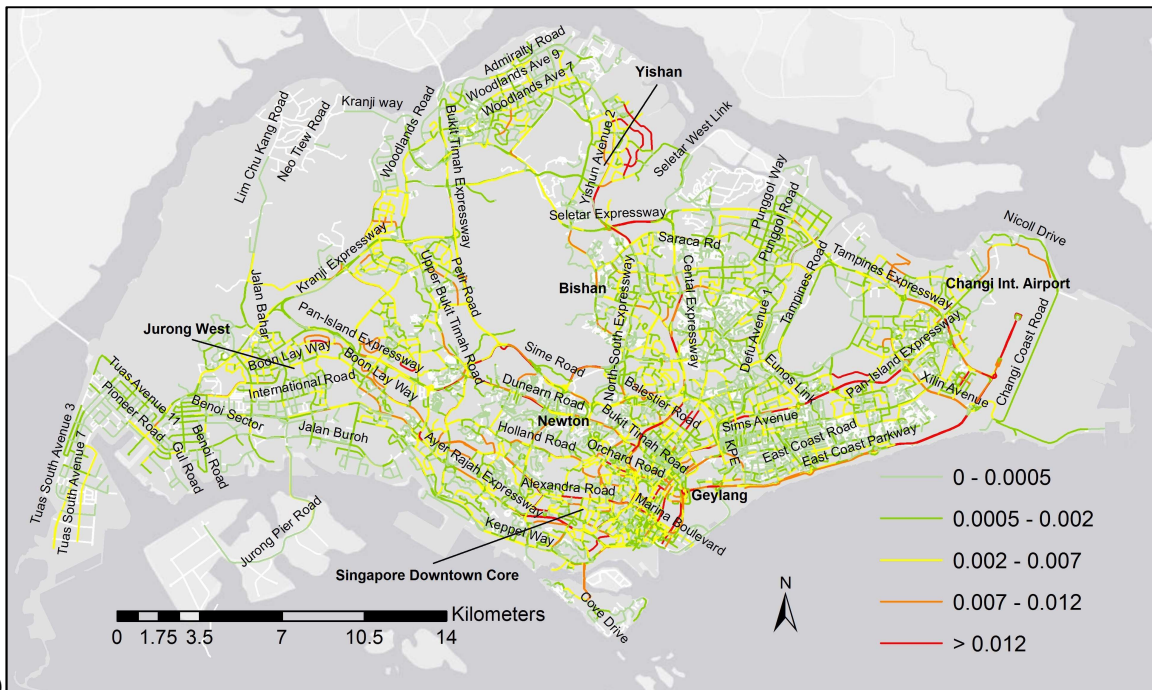
382



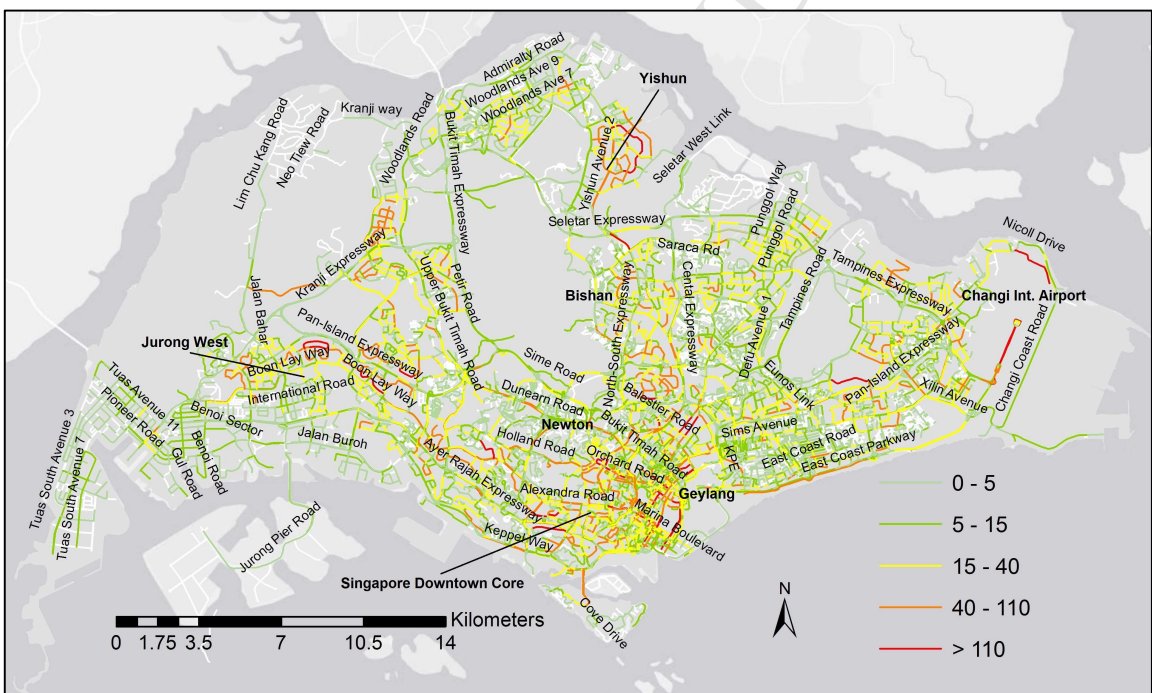
383

(a)

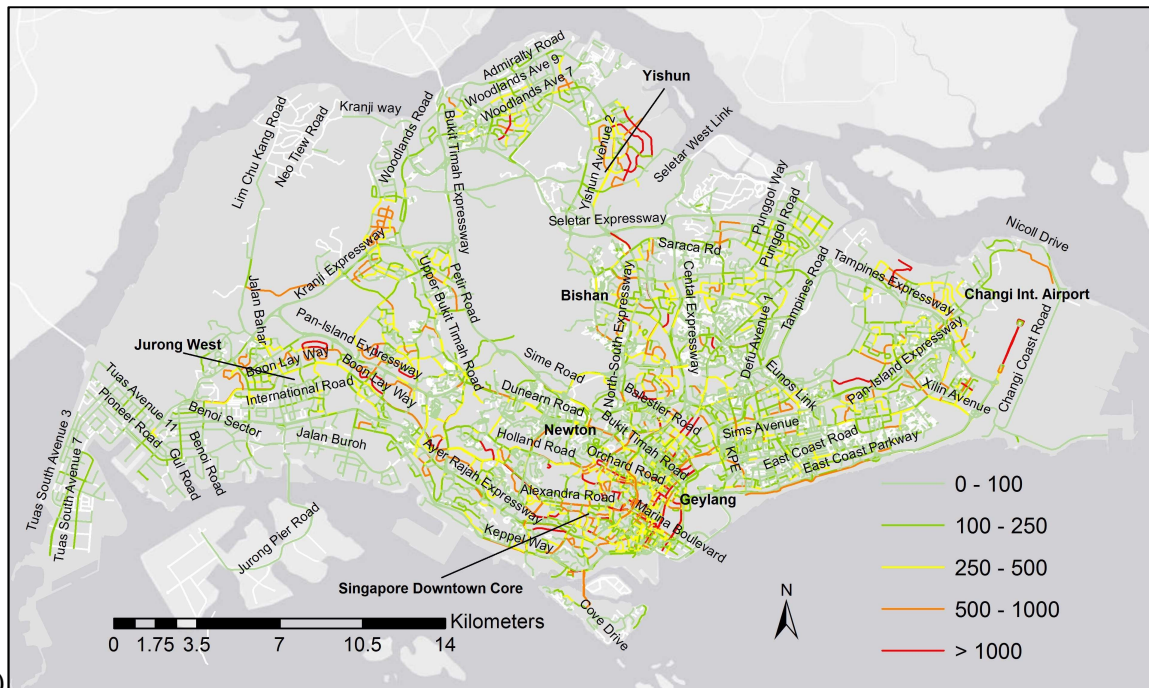




384 (b)



385 (c)



386 (d)  
 387 **Figure 4.** Spatial distributions of predicted daily emissions from the vehicle fleet for each  
 388 road link for the parameters of (a) CO<sub>2</sub> (tonnes/day), (b) NO<sub>x</sub> (tonnes/day), (c) VOC (g/day),  
 389 and (d) PM (g/day) in Singapore on the 23<sup>rd</sup> February 2011. Locations of relatively high-  
 390 emissions, are observed in the Singapore Downtown Core area in the south-center of  
 391 Singapore and in other locations throughout the island.

392  
 393

394 The locations where predicted emissions were relatively higher across Singapore can be  
 395 identified for the four pollution parameters of CO<sub>2</sub>, NO<sub>x</sub>, VOC and PM. In terms of CO<sub>2</sub>  
 396 emissions, the areas which were identified as having relatively higher CO<sub>2</sub> output from the  
 397 vehicle fleet. Marina South and Raffles Place in the Downtown Core area, the Harbour Front  
 398 area, Jurong East, Clementi, Sin Ming and an area close to the Seletar Reservoir in Yishun  
 399 were identified. In the east of Singapore, the area between Tampines and Changi International  
 400 Airport was identified as having relatively higher CO<sub>2</sub> emissions than other areas. The Bukit  
 401 Timah Road - Whitley Road Intersection was selected as having relatively higher CO<sub>2</sub>  
 402 emissions as were the busy areas Novena, Newton, Somerset, Dhoby Ghaut (north) and  
 403 Farrer Park which are located north of the central region of Singapore.

404

405 Relatively higher levels of NO<sub>x</sub> emissions were predicted in the Downtown Core Area such  
 406 as in Chinatown, Outram Park, Clarke Quay and Raffles Place. The Chin Swee Tunnel -  
 407 Havelock Road intersection area was also identified. North of Dhoby Ghaut, City Hall, on the

408 Central Expressway side of Fort Canning Park and Little India were areas where relatively  
409 higher NO<sub>x</sub> emissions were predicted. Connected to these, Somerset and Orchard were areas  
410 with relatively higher NO<sub>x</sub> emissions. The Moulmein Flyover, the Jalan Bukit Merah - Lower  
411 Delta Road Intersection (located west of the Downtown Core area), the Kallang-Paya Lebar  
412 Expressway (KPE) - Nicoll Highway Intersection (located east of the Downtown Core area),  
413 and further east, an area in the vicinity of Changi International Airport was also identified.  
414 For VOC emissions, the areas of elevated emissions were observed to be centrally located  
415 with a few areas scattered in other parts of Singapore. Located centrally were Orchard Road,  
416 the River Valley Road - Zion Road Intersection, Outram Park, Marina South, Suntec City and  
417 Little India. Moving east from the urban central region - Selegie, Lavender, Kallang,  
418 Geylang, and further east, the Layang Avenue - Pasir Ris Drive 1 Intersection and the Pan  
419 Island Expressway (PIE) - Tampines Expressway (TPE) Intersection near Changi  
420 International Airport were identified as hotspots for VOC emissions. North-east of the central  
421 region was Tao Payoh and further north was Sin Ming (Yishun area). Westwards from the  
422 Downtown Core areas were Bukit Merah, the Holland Road - Farrer Road Intersection.  
423 Further west was Clementi, Jurong East and Bukit Batok. In the north-west of Singapore,  
424 Choa Chu Kang was observed to have relatively higher levels of VOC.

425  
426 For PM emissions, all the areas of relatively highest predicted emissions were concentrated in  
427 the Downtown Core area with some areas identified to the east of it. The areas identified  
428 included the areas of Outram Park, Chinatown, Raffles Place and Clarke Quay. South of these  
429 the Tajang Pagar area near Keppel Road was chosen and slightly north of these, the Havelock  
430 Road - Outram Road Intersection. River Place near the Chin Swee Tunnel and the Central  
431 Expressway side of Fort Canning Park were identified. On the east of the Downtown Core  
432 area were Bugis, Beach Road and Geylang. On the west side of the Downtown Core area; the  
433 Jalan Bukit Merah - Lower Delta Road Intersection was included in the selection of areas  
434 determined to have increased PM emissions relative to the rest of the island. Other areas were  
435 the extent of Orchard Road, Farrer Park and Balestier.

436  
437

### 438 ***3.2. Comparison of predicted emissions for the total motor vehicle population***

439

440 Total emissions of each pollutant parameter for the vehicle fleet studied were computed for  
441 each day and the means determined are presented in Table 2. The mean daily CO<sub>2</sub> and NO<sub>x</sub>

442 emissions determined were respectively representative of 7.9% ( $\pm 3\%$ ) and 7.6% ( $\pm 1.4\%$ ) of  
443 emissions estimates for the total motor vehicle population of Singapore (including the  
444 previously calculated vehicle fleet emissions). For VOC and PM, the proportions were  
445 smaller, whereas the total daily emissions computed were approximately 3.2% ( $\pm 1.7\%$ ) and  
446 3.5% ( $\pm 1.6\%$ ) (respectively) of total motor vehicle population emissions (see Table 2 for  
447 details).

448  
449 Daily emissions from the total motor vehicle population were then computed for one week  
450 and compared to other transportation emissions estimated by Streets and Lu (2012) (see Table  
451 3). The overall emissions levels computed for the entire fleet were comparable to those  
452 attained from Streets and Lu (2012). Whereas our analyses predicted mean daily emissions  
453 from the entire motor vehicle population to be 27656 ( $\pm 3049$ ) tonnes for CO<sub>2</sub>, Streets and Lu  
454 computed 24417 tonnes/day. Therefore, the relative difference in emissions was found to be  
455 15% ( $\pm 1.7\%$ ). For NO<sub>x</sub> we determined total daily emissions to be 155 ( $\pm 33.1$ ) tonnes/day  
456 while Streets and Lu computed 121 tonnes/day, and this corresponded to a relative difference  
457 of 24% ( $\pm 4.9\%$ ). A larger disparity was observed in the case of VOC. We predicted total  
458 emissions to be 9.7 ( $\pm 2.6$ ) tonnes/day whereas Streets and Lu determined a value of 21.6  
459 tonnes/day. This is equivalent to a relative difference of -49% ( $\pm 12.3\%$ ). Finally, for PM we  
460 computed 8.5 ( $\pm 3.4$ ) tonnes/day while Streets and Lu predicted 14.1 tonnes/day. Similar to  
461 VOC, we calculated a relatively lower value to Streets and Lu by 39% ( $\pm 15.5\%$ ), but  
462 exhibiting a larger uncertainty.

463  
464

465 **Table 2.** Modeled emissions for the taxi fleet and the proportion of modeled taxi emissions in  
 466 the estimated total motor vehicle population emissions, for each of four air pollutant  
 467 parameters.

	<b>Modeled Emissions Taxi Fleet</b>	<b>Proportion of Modeled Taxi Emissions in the Total Motor Vehicle Population Emissions</b>
	<b>(tonnes/day)</b>	<b>%</b>
	<b>Mean (SD)</b>	<b>Mean (SD)</b>
<b>CO<sub>2</sub></b>	2176.6 (1023.5)	7.9 (3.0)
<b>NO<sub>x</sub></b>	11.9 (2.8)	7.6 (1.4)
<b>VOC</b>	0.3 (0.2)	3.2 (1.7)
<b>PM</b>	0.3 (0.2)	3.5 (1.6)

468

469

470 **Table 3.** Comparison of the mean daily emissions predicted for the total motor vehicle  
 471 population of Singapore to estimated ground transportation emissions attained from Streets  
 472 and Lu (2012).

	<b>Predicted Total Motor Vehicle Population Emissions</b>	<b>Streets and Lu (2012)</b>		
	<b>(tonnes/day)</b>	<b>(tonnes/day)</b>		
	<b>Mean (SD)</b>	<b>Mean</b>	<b>Range of Ratios</b>	<b>Average difference (SD) (%)</b>
<b>CO<sub>2</sub></b>	27656 (3049)	24417	(1.1-1.3)	15.1 (1.7)
<b>NO<sub>x</sub></b>	155.2 (33.1)	121	(1.0-1.6)	24.1 (4.9)
<b>VOC</b>	9.7 (2.6)	21.6	(0.4-0.7)	-49.3 (12.3)
<b>PM</b>	8.5 (3.4)	14.1	(0.4-0.8)	-38.7 (15.5)

473

474

475

476



#### 477 4. Discussion

478

479

480 Recent advances in urban computing and the availability of large transportation GPS datasets  
481 have presented new opportunities for real-time transportation and emissions modeling.  
482 Transportation and emissions modeling conducted in previous studies have been limited by  
483 coarsely resolved predicted or measured traffic information. In this study, we analyzed GPS  
484 traces from a fleet of over 15,000 vehicles in Singapore with the aim of using this  
485 information to make predictions of emissions in high spatial resolution throughout the study  
486 domain. The instantaneous velocities and accelerations of vehicles, which were extracted in  
487 high spatial and temporal resolution, were inputted into a microscopic emissions model. The  
488 air pollution emissions of CO<sub>2</sub>, NO<sub>x</sub>, VOC and PM were thus quantified. The spatial  
489 distributions of the emissions were examined and this enabled highly localized areas of  
490 elevated emission levels to be identified. The study demonstrated how instantaneous drive  
491 cycles can be used to predict vehicular pollutant emissions and this forms an important  
492 component of the urban emissions inventory.

493

494 An analyses demonstrated that the taxi data could be used to predict overall traffic volumes  
495 on road segments throughout the road network. Emissions from the taxi fleet and then the  
496 total motor vehicle population were therefore predicted for the study domain of Singapore.  
497 The subsequent emissions levels computed for the entire motor vehicle population was  
498 comparable to those attained from Streets and Lu (2012). Whereas the modeled values are in  
499 the same order of magnitude for each pollutant parameter, the results likely varied due to the  
500 different emissions modeling methods employed. Further to this, in the case of Streets and Lu  
501 (2012) estimates of emissions from the transportation sector are from the year 2012, while  
502 our data are representative of one week of data for the year 2011. Predicted emissions  
503 computed for CO<sub>2</sub> and NO<sub>x</sub> were higher than VOC and PM. The reason for this is that the  
504 emissions function parameters used are higher for CO<sub>2</sub> and NO<sub>x</sub>. CO<sub>2</sub> and PM emission  
505 estimates are more sensitive to vehicle velocities than VOC and NO<sub>x</sub> which are more  
506 sensitive to accelerations (Int Panis et al., 2006).

507

508 This paper presents a novel methodology for making instantaneous emission modeling  
509 compatible with microscopic traffic patterns (measured on a second by second basis).  
510 Previous studies have focused on the microscopic traffic simulation coupled with

511 microscopic emissions modeling (Int Panis et al., 2006) or a combination of macroscopic and  
512 microscopic traffic simulation combined with microscopic emissions modeling (Osorio and  
513 Nanduri, 2015). However, to the authors knowledge, a study investigating measured  
514 microscopic vehicle movement (measured on a second by second basis using GPS) in tandem  
515 with microscopic emissions modeling has not been completed successfully for a substantially  
516 sized vehicle fleet and study domain, rather have been limited to small ad hoc deployments.

517

518 The methodology described in this study has the potential to inform environmental policy  
519 related to transportation in urban areas. With the framework proposed, where appropriate data  
520 is available, responsive and adaptive strategies could be implemented should the emissions  
521 model be applied using real-time GPS data. The methodology described demonstrated the  
522 potential for linking GPS measured vehicle movements directly with microscopic emissions  
523 models (based on the instantaneous driving speed and acceleration) for quantifying traffic  
524 emissions. Although the computation of emissions is clearly a useful application, it is in the  
525 implementation and evaluation of real-time, technology-based environmental policies related  
526 to transportation where its application would be most beneficial. Technologies for monitoring  
527 and controlling vehicle velocities include Intelligent Speed Adaption (ISA) systems  
528 (Duynstee et al., 2001; Int Panis et al., 2006). ISA systems are electronic systems installed in  
529 vehicles, which utilize GPS navigation to evaluate the vehicle location and apply appropriate  
530 speed limits on specific road segments ISA systems combined with an appropriate real-time  
531 emissions model could be utilized for minimizing emissions and fuel consumption in urban  
532 road networks in the future.

533

534 Environment related transportation policies such as restricting vehicles in a city-center zone  
535 or restricting odd/even number plates in urban regions have been adopted in a number of  
536 cities in recent years (Fensterer et al., 2014; Holman et al., 2015). Whereas these have helped  
537 in the reduction of congestion and pollution levels in urban centers, more beneficial  
538 approaches may be based on the detection of the specific, fixed positions where emissions  
539 take place, rather than in substantial urban regions. With the dynamic fine grain emissions  
540 inventory presented in this study, it may become feasible to target air pollution emissions  
541 mitigation efforts in a far more direct manner. The health and economic benefits of reducing  
542 air pollution emissions across various sectors including transportation, thereby improving air  
543 quality, has been quantified in many reports. For example, the US EPA computed the costs  
544 for the implementation of the 1990 Clean Air Act to be about 65 million dollars, with a

545 potential benefit reaching 2 trillion dollars from 1990 to 2020, potentially avoiding  
546 approximately 230,000 premature deaths in 2020 (USEPA, 2011).

547

548 For the first time, the data collected allow us to see an emission inventory not as something  
549 static which only changes from one road segment to the other, but which has more detailed  
550 characteristics with spatiotemporal variation. This enables a better estimate of the impact of  
551 pollution on the urban population which also exhibits variable spatial and temporal  
552 distribution profiles over the course of the day (Nyhan et al., forthcoming). The advantage of  
553 the proposed method is that by interrogating and interpreting easily accessible data from  
554 existing fleets (such as vehicle or bus services), considerable information regarding air  
555 pollution emissions can be obtained at a low cost and minimal effort in cities. Such a system  
556 can be applied in other cities, perhaps through government encouragement to make  
557 transportation GPS data available. This information may be of considerable value in  
558 determining the most appropriate locations of where to take action to reducing emissions and  
559 subsequently air pollution concentration levels in cities. This type of data could also be used  
560 to compute fine-grained fuel consumption patterns from the transportation sector.

561

562 This approach we adopted for predicting emissions has some limitations. In the development  
563 of the emissions model functions, Int Panis et al., (2006) primarily used measurements made  
564 in urban traffic (with low speeds) for determining functional forms and the variables in the  
565 emissions equations used in this study. This is considered sufficient for the purposes of  
566 evaluating the effects of speed management in urban networks. It is possible that the emission  
567 functions for highway traffic (at higher speeds) differ for those of urban traffic and the traffic  
568 on highways was insufficiently represented in the functions used. The emissions model did  
569 not allow for the specific model or age of the vehicles to be considered in computations  
570 either. Some additional measures would also be needed to verify the quality of the  
571 acceleration data obtained from GPS traces. There are inherent inaccuracies associated with  
572 GPS measurements, which however are compensated by the large volume of data collected.  
573 There is a necessity to connect the movements of the subset of vehicles with the movement of  
574 all the vehicles in the city. For this, calibrations parameters could be applied based on the  
575 sampling of the available vehicles versus the total number of vehicles. Finally, additional  
576 work would be needed to link the emissions predicted for various parameters to local  
577 measured air pollution concentration levels. A future study by these authors will therefore



578 examine the relationship between predicted emissions using the methodology described  
579 herein this study, and measured or modeled values of air pollution concentrations.

580

581 This methodology described in this paper may be replicated in a number of cities worldwide,  
582 as GPS traces from vehicles become increasingly available. Vehicle fleet operators can do a  
583 major public service by providing GPS data for research, in particular for predicting  
584 emissions and other information relevant to environmental health from it. This information  
585 may be used for designing air pollution intervention strategies (long-term, short-term,  
586 responsive and adaptive) for the protection of human health and well-being.

587

588

## 589 **5. Conclusions**

590

591 Through analyzing GPS data from a large transportation fleet in Singapore, fine grained  
592 emissions were estimated in high spatial resolution. The emissions model was based on the  
593 inputs of velocity and acceleration parameters extracted from the data. Air pollution  
594 emissions related to CO<sub>2</sub>, NO<sub>x</sub>, VOC and PM were thereby quantified. The spatial  
595 distributions of the emissions were investigated thereby enabling highly localized areas of  
596 relatively higher emissions levels to be identified. This study also shows how the  
597 instantaneous drive cycles can be applied in the estimation of the overall emissions from the  
598 transportation sector within the study area.

599

## 600 7. Acknowledgements

601

602 All the authors wish to thank the MIT SENSEable City Lab Consortium and the Singapore-  
603 MIT Alliance for Research & Technology program for supporting the research. M. Nyhan  
604 would like to thank Fulbright and the Irish Environmental Protection Agency. The authors  
605 would also like to acknowledge Dr. Luc Int. Panis for providing advice on some modeling  
606 aspects of the study.

607

608

609

## 610 8. References

611

612 Akimoto, H., 2003. Global Air Quality and Pollution. *Science* 302, 1716-1719.

613

614 An, F., Barth, M., Ross, M., Norbeck, J., 1997. The development of a comprehensive modal  
615 emission model: operating under hot-stabilize conditions. *Transportation Research Record*.  
616 1587, 52-62.

617

618 Aslam, J., Lim, S., Pan, X., Rus, D., 2012. City-scale traffic estimation from a roving sensor  
619 network. *SenSys' 12*, November 6-9, 2012. ACM 978-1-1169-4.

620

621 Barth, M., Scora, G., 2006. *Comprehensive Modal Emission Model (CMEM), version 3.01*  
622 *User's Guide*. Riverside: University of California.

623

624 Bell, M.L., Davis, D.L., Fletcher, T., 2004. A Retrospective Assessment of Mortality from the  
625 London Smog Episode of 1952: The Role of Influenza and Pollution; *Environmental Health*  
626 *Perspectives*. 112, 6-8.

627

628 Ben-Akiva, M., Koutsopoulos, H.N., Mishalani, R., Yang, Q., 1997. Simulation laboratory  
629 for evaluating dynamic traffic management systems. *Journal of Transportation Engineering*.  
630 123(4), 283-289.

631

632 Britter, R. E., and Hanna, S. R., 2003. Flow and dispersion in urban areas. *Annual Review of*  
633 *Fluid Mechanics*. 35, 469-496.

- 634  
635 Burke, J. A., Estrin, D., Hansen, M., Parker, A., Ramanathan, N., Reddy, S., and Srivastava,  
636 M. B., 2006. Participatory Sensing. UC Los Angeles: Center for Embedded Network Sensing.  
637 Retrieved from <<http://escholarship.org/uc/item/19h777qd>>  
638
- 639 Caiazzo, F., Ashok, A., Waitz, I.A., Yim, S.H.L., and Barrett, S.R.H., 2013. Air pollution and  
640 early deaths in the United States. Part I: Quantifying the impact of major sectors in 2005.  
641 Atmospheric Environment. 79, 198-208.  
642
- 643 Campbell, A. T., Eisenman, S. B., Lane, N. D., Miluzzo, E., Peterson, R. A., Lu, H., Zheng,  
644 X., Musolesi, M., Fodor, K. and Ahn, G-S., 2008. The Rise of People-Centric Sensing. IEEE  
645 Internet Computing. 12, 12-21.  
646
- 647 Canagaranta, M. R., Jayne, J. T., Ghertner, D. A., Herndon, S., Shi, Q., Jimenez, J. L., Silva,  
648 P. J., Williams, P., Lanni, T., Drewnick, F., Demerjian, K. L., Kolb, C. E., and Worsnop, D.  
649 R., 2004. Case studies of particulate emissions from in-use New York City vehicles. Aerosol  
650 Science and Technology. 38, 555-573.  
651
- 652 CERC, 2015. ADMS Urban, Cambridge Environmental Research Consultants, Cambridge,  
653 United Kingdom.  
654
- 655 Chong, C-Y. and Kumar, S. P., 2003. Sensor networks: evolution, opportunities and  
656 challenges. Proceedings of the IEEE. 91, 1247-1256.  
657
- 658 Cuff, D., Hansen, M., and Kang, J., 2008. Urban sensing: out of the woods. Communications  
659 of the ACM. 51, 24-33.  
660
- 661 Duynstee, L., Katteler, H., Martens, A. Intelligent speed adaptation: selected results of the  
662 practical trial. Proc. 8th world congress on intelligent transport systems, Sydney, Australia, 30  
663 September-4 October, 2001.  
664
- 665 El-Sgawarby, I., Kyoungcho, A., Rakha, H., 2005. Comparative field evaluation of vehicle  
666 cruise speed and acceleration levels impacts on hot stabilized emissions. Transportation  
667 Research. 10D, 13-30.

668  
669 Fecht, D., Hansell, A.L., Morley, D., Dajnak, D., Vienneau, D., Beevers, S., Toledano, M.B.,  
670 Kelly, F.J., Anderson, H.R., Gulliver, J., 2016. Spatial and temporal associations of road  
671 traffic noise and air pollution in London: Implications for epidemiological studies.  
672 *Environment International*. 88, 235-242.  
673  
674 Fensterer, V., Kuchenhoff, H., Maier, V., Wichmann, H.-E., Breitner, S., Peters, A., Gu, J.,  
675 Cyrus, J., 2014. Evaluation of the impact of low emission zone and heavy traffic-ban in  
676 Munich (Germany) on the reduction of PM<sub>10</sub> in ambient air. *International Journal of*  
677 *Environment and Public Health*. 11(5), 5094-5112.  
678  
679 Fontes, T., Pereira, S.R., Fernandes, P., Bandeira, J.M., Coelho, M.C., 2015. How to combine  
680 different micro-simulation tools to assess the environmental impacts of road traffic? Lessons  
681 and directions. *Transportation Research Part D*. 34, 293-306.  
682  
683 Frey, H. C., Unal, A., Roupail, N. M. and Colyar, J. D., 2003. On-road measurement of  
684 vehicle tailpipe emissions using a portable instrument. *Journal of the Air & Waste*  
685 *Management Association*. 53, 992–1002.  
686  
687 Fruin, S., Westerdahl, D., Sax, T., Sioutas, C., Fine, P.M., 2008. Measurements and predictors  
688 of on-road ultrafine particle concentrations and associated pollutants in Los Angeles.  
689 *Atmospheric Environment*. 42(2), 207-219.  
690  
691 González, M.C., Hidalgo, C.A., Barabási, A.L., 2008. Understanding individual human  
692 mobility patterns. *Nature*. 453, 779–782.  
693  
694 Grauwil, S., Sobolevsky, S., Moritz, S., Godor, I., Ratti, C., 2014. Towards a comparative  
695 science of cities: using mobile traffic records in New York, London and Hong Kong.  
696 *Computational Approaches for Urban Environments, Geo-technologies and the Environment*.  
697 13, 363–387.  
698  
699 Gurhar, B.R., Jain, A., Sharma, A., Agarwal, A., Gupta, P., Nagpure, A.S. Lelieveld, J., 2010.  
700 Human health risks in megacities due to air pollution. *Atmospheric Environment*. 44, 4606-  
701 4613.

- 702  
703 Guzella, L. and Sciarreta, A., 2005. Vehicle propulsion systems: introduction to modeling and  
704 optimization. Springer Verlag.  
705
- 706 Holman, C., Harrison, R., Querol, X., 2015. Review of the efficacy of low emission zones to  
707 improve urban air quality in European cities. *Atmospheric Environment*. 111, 161-169.  
708
- 709 Hoteit, S., Secci, S., Sobolevsky, S., Ratti, C., Pujolle, G., 2014. Estimating human  
710 trajectories and hotspots through mobile phone data. *Computer Networks*. 64, 296-307.  
711
- 712 Hu, T.-Y., and Mahmassani, H.S., 1997. Day-to-day evolution of network flows under real-  
713 time information and reactive signal control. *Transportation Research*. 5C(1), 51-69.  
714
- 715 Int Panis, L., Broekx, S., Liu, R., 2006. Modeling instantaneous traffic emission and the  
716 influence of traffic speed limits. *Science of the Total Environment*. 371, 270-285.  
717
- 718 Jerrett, M., Burnett, R.T., Ma, R., Pope, C.A., III, Krewski, D., Newbold, K.B., Thurston, G.,  
719 Shi, Y., Finkelstein, N., Calle, E.E., Thun, M.J., 2005. Spatial Analysis of Air Pollution and  
720 Mortality in Los Angeles. *Epidemiology*. 16, 727-736.  
721
- 722 Kang, C., Sobolevsky, S., Liu, Y., Ratti, C., 2013. Exploring human movements in Singapore:  
723 A comparative analysis based on mobile phone and taxicab usages. In *Proceedings of the 2nd*  
724 *ACM SIGKDD International Workshop on Urban Computing* (p. 1). ACM.  
725
- 726 Kumar, P., Morawska, L., Martani, C., Biskos, G., Neophytou, M., Di Sabatino, S., Bell, M.,  
727 Norford, L., Britter, R., 2015. The rise of low-cost sensing for managing air pollution in  
728 cities. *Environment International*. 75, 199-205.  
729
- 730 Kung, K.S., Greco, K., Sobolevsky, S., Ratti, C., 2014. Exploring universal patterns in human  
731 home-work commuting from mobile phone data. *PLoS ONE*. 9(6): e96180.  
732 doi:10.1371/journal.pone.0096180  
733
- 734 Krewski, D., Jerrett, M., Burnett, R.T., Ma, R., Hughes, E., Shi, Y., Turner, M.C., Pope, C.A.  
735 3rd, Thurston, G., Calle, E.E., Thun, M.J., Beckerman, B., DeLuca, P., Finkelstein, N., Ito,

- 736 K., Moore, D.K., Newbold, K.B., Ramsay, T., Ross, Z., Shin, H., Tempalski, B., 2009.  
737 Extended follow-up and spatial analysis of the American Cancer Society study linking  
738 particulate matter and mortality. Research Report from the Health Effects Institute: 5-114;  
739 Discussion 115-136.  
740
- 741 Laden, F., Schwartz, J., Speizer, F.E., Dockery, D.W., 2006. Reduction in fine particulate air  
742 pollution and mortality extended follow-up of the Harvard six cities study. American Journal  
743 of Respiratory and Critical Care Medicine. 173, 667-672.  
744
- 745 Land Transport Authority of Singapore, 2015. Transportation fleet composition datasets  
746 available at <data.gov.sg>  
747
- 748 Laxen, D., Wilson, P., Marner, B., Moorcroft, S., and Brown Y., 2003. Review of Air Quality  
749 Monitoring in London. Report for the Mayor, the Association of London Government (ALG)  
750 and the Department for Environment Food and Rural Affairs (DEFRA). Air Quality  
751 Consultants: Bristol.  
752
- 753 Lewtas, J., 2007. Air pollution combustion emissions: Characterization of causative agents  
754 and mechanisms associated with cancer, reproductive, and cardiovascular effects. Mutation  
755 Research. 636, 95-133.  
756
- 757 Liu, R., van Vliet, D., Watling, D., 2006. Micro-simulation models incorporating both  
758 demand and supply dynamics. Transportation Research. 40A(2), 125-50.  
759
- 760 Mantazeri-Gh, M. and Naghizadeh, M., 2003. Development of car drive cycle for simulation  
761 of emissions and fuel economy. Proceedings of the 15<sup>th</sup> European Simulation Symposium. 1-  
762 6.  
763
- 764 Metric Mind Corporation, 2012. Data drive cycles. Retrieved from  
765 <<http://www.metricmind.com/data/cycles.pdf>>  
766
- 767 Molina, L. T., Molina, M. J., Slott, R. S., Kolb, C. E., Gbor, P. K., Meng, F., Singh, R. B.,  
768 Galvez, O., Sloan, J. J., Anderson, W. P., Tang, X., Hu, M., Xie, S., Shao, M., Zhu, T., Zhang,  
769 Y. H., Gurjar, B. R., Artaxo, P. E., Oyola, P., Gramsch, E., Hidalgo, D., and Gertler, A. W.,

- 770 2004. Air Quality in Selected Megacities. *Journal of the Air & Waste Management*  
771 *Association*. 54(12), 1-73.
- 772
- 773 Molina, M. J. and Molina, L. T., 2004. Megacities and atmospheric pollution. *Journal of Air*  
774 *and Waste Management*. 54, 644-680.
- 775
- 776 Moretti, F., Pizzuti, S., Panzieri, S., Annunziato, M., 2015. Urban traffic flow forecasting  
777 through statistical and neural network bagging ensemble hybrid modeling. *Neurocomputing*,  
778 167, 3-7.
- 779
- 780 NARSTO, 2005. Improving emission inventories for effective air quality management across  
781 North America. NARSTO 05-001. Pasco, Washington, USA.
- 782
- 783 NEA (National Environment Agency), 2015. Available at <[www.nea.gov.sg](http://www.nea.gov.sg)>
- 784
- 785 North, R. J., Noland, R. B., Ochieng, W. Y., and Polak, J. W., 2006. Modeling of particulate  
786 matter mass emissions from a light-duty diesel vehicle. *Transportation Research Part D:*  
787 *Transport and Environment*. 11, 344-357.
- 788
- 789 Nyhan, M., Misstear, B.D., McNabola, A., 2014a. Comparison of particulate matter dose and  
790 acute heart rate variability response in cyclists, pedestrians, bus and train passengers. *Science*  
791 *of the Total Environment*. 468-469, 821-831.
- 792
- 793 Nyhan, M., Misstear, B., McNabola, A., 2014b. Evaluating artificial neural networks for  
794 predicting minute ventilation and lung deposited dose in commuting cyclists. *Journal of*  
795 *Transport & Health*. 1(4), 305-315.
- 796
- 797 Nyhan, M., Britter, R., Grauwlin, S., Laden, F., McNabola, A., Misstear, B., Ratti, C.,  
798 forthcoming. Exposure Track – the impact of mobile device based mobility patterns on  
799 quantifying population exposure to air pollution.
- 800
- 801 Osorio, C., Nanduri, K., 2015. Urban transportation emissions mitigation: Coupling high-  
802 resolution vehicular emissions and traffic models for traffic signal optimization.  
803 *Transportation Research Part B*. Accepted and in press.

- 804  
805 Paulos, E., Honicky, R.J., and Hooker, B., 2009. Citizen Science: Enabling Participatory  
806 Urbanism. In Foth, M. (Ed.) *Urban Infomatics: The practice and promise of the real-time city*.  
807 IGI Global, Hershey, PA.  
808
- 809 Parkinson B.W., 1996. GPS error analysis, *Global Positioning System: Theory and*  
810 *applications*. Progress in Astronautics and Aeronautics. 163, 469-483.  
811
- 812 Pei, T., Sobolevsky, S., Ratti, C., Shaw, S.L., Li, T., Zhou, C., 2014. A new insight into land  
813 use classification based on aggregated mobile phone data. *International Journal of*  
814 *Geographical Information Science*. 28(9) p.1-20.  
815
- 816 Pelkmans, L., Debal, P., Hood, T., Hauser, G., Delgado, M.R., 2004. Development of a  
817 simulation tool to calculate fuel consumption and emissions of vehicles operating in dynamic  
818 conditions. SAE 2004 spring fuels and lubricants, 2004-01(1873). Warrendale PA, (USA):  
819 SAE International (Society of Automotive Engineers).  
820
- 821 Rakha, H., Kyounga, A., Trani, A., 2004. Development of a VT-Micro model for estimating  
822 hot stabilized light-duty vehicle and truck emissions. *Transportation Research*. 9D, 49-74.  
823
- 824 Samuel, S., Austin, L. and Morrey, D., 2002. Automotive test drive cycles for emission  
825 measurement and real-world emission levels- a review. *Proceedings of the Institution of*  
826 *Mechanical Engineers, Part D: Journal of Automobile Engineering*. 216, 555-564.  
827
- 828 Santi, P., Resta, G., Szell, M., Sobolevsky, S., Strogatz, S., Ratti, C., 2014. Quantifying the  
829 benefits of vehicle pooling with sharability networks. *Proceedings of the National Academy*  
830 *of Sciences*. 111(37), 13290-13294.  
831
- 832 Singapore Department of Statistics, 2015. *Yearbook of Statistics Singapore 2015*. Available at  
833 <[www.singstat.gov.sg](http://www.singstat.gov.sg)>  
834
- 835 Shorter, J., Herndon, S., Zahniser, M. S., Nelson, D. D., Womrhoudt, J., Demerjian, K. L. and  
836 Kolb, C. E., 2005. Real-time measurements of nitrogen oxide emissions from in-use New



- 837 York City transit buses using a chase vehicle. *Environmental Science and Technology*. 39,  
838 7991- 8000.  
839
- 840 Sobolevsky, S., Szell, M., Campari, R., Couronné, T., Smoreda, Z., Ratti, C., 2013.  
841 Delineating geographical regions with networks of human interactions in an extensive set of  
842 countries. *PLoS ONE*. 8(12), e81707 doi: 10.1371/journal.pone.0081707.  
843
- 844 Streets, D., Lu, Z., 2012. Anthropogenic emissions inventory for 5 major sectors for South  
845 East Asia and China. Argonne National Laboratory for the National Aeronautics and Space  
846 Administration (NASA) SEAC4RS project.  
847
- 848 Thiagarajan, A., Ravindranath, L., LaCurts, K., Madden, S., Balakrishnan, H, Toledo, S. and  
849 Eriksson, J., 2009. VTrack: Accurate, energy-aware road traffic delay estimation using  
850 mobile phones. *SenSys'09*, Berkley, CA, USA.  
851
- 852 USEPA (United States Environmental Protection Agency), 2009. AERMOD Modeling  
853 System. Available at [www.epa.gov](http://www.epa.gov)  
854
- 855 USEPA (United States Environmental Protection Agency), 2011. The Benefits and Costs of  
856 the Clean Air Act from 1990 to 2020. Final Report-Rev. A. US Environmental Protection  
857 Agency Office for Air and Radiation.  
858
- 859 USEPA (United States Environmental Protection Agency), 2012. MOBILE Model  
860 documentation. Available at [www.epa.gov](http://www.epa.gov)  
861
- 862 Vardoukalis, S., Gonzalez-Flesca, N., Fisher, B. E. A., and Pericleous, K., 2005. Spatial  
863 variability of air pollution in the vicinity of a permanent monitoring station in central Paris.  
864 *Atmospheric Environment*. 39, 2725-2736.  
865
- 866 WHO (World Health Organization), 2014. Urban Population Growth, Global Health  
867 Observatory. Available at [www.who.int](http://www.who.int)  
868

869 WHO (World Health Organization), 2014. Burden of disease from ambient air pollution for  
870 2012. Available at <[www.who.int](http://www.who.int)>

871

872 Zhang, J. and Morawska, L., 2002. Combustion sources of particles: 2. Emission factors, and  
873 measurement methods. *Chemosphere*. 49, 1059-1074.

874

875

ACCEPTED MANUSCRIPT

876 *List of Tables*

877 **Table 1.** Motor vehicle population in Singapore by category and type of fuel used for the year  
878 2011. Figures exclude tax exempted vehicles for off-the-road use (RU plates).

879

880 **Table 2.** Modeled emissions for the taxi fleet and the proportion of modeled taxi emissions in  
881 the estimated total motor vehicle population emissions, for each of four air pollutant  
882 parameters.

883

884 **Table 3.** Comparison of the mean daily emissions predicted for the total motor vehicle  
885 population of Singapore to estimated ground transportation emissions attained from Streets  
886 and Lu (2012).

887

888 *List of Figures*

889 **Figure 1.** Distribution of traffic volumes (i.e. number of vehicles per road segment) on 15  
890 randomly selected road segments for the 23rd February 2011. The x-axis includes 15 road  
891 segments including a point for every 15 minutes during the 24-hour day. The y-axis  
892 represents the percentage of traffic at that location and time. The taxi distribution (in blue)  
893 underestimates the loop distribution (in green) and the underestimation is variable.

894

895 **Figure 2.** Results of the feed-forward artificial neural network model implementation.  
896 Regression plot of a partial set of modeled traffic volumes versus corresponding measured  
897 traffic volume for the (a) training phase ( $R^2=96\%$ ), (b) validation phase ( $R^2=93\%$ ), (c) testing  
898 phase ( $R^2=92\%$ ) and (d) overall model ( $R^2=94\%$ ). A sub-sample of points are presented for  
899 clarity.

900

901 **Figure 3.** Spatial distribution of the number of valid accelerations in Singapore on the 23<sup>rd</sup>  
902 February 2011. Locations where relatively higher numbers of valid accelerations are  
903 observed in the vicinity of the Singapore Downtown Core area and the Changi International  
904 Airport in the east.

905

906 **Figure 4.** Spatial distributions of predicted daily emissions from the vehicle fleet for each  
907 road link for the parameters of (a) CO<sub>2</sub> (tonnes/day), (b) NO<sub>x</sub> (tonnes/day), (c) VOC (g/day),  
908 and (d) PM (g/day) in Singapore on the 23<sup>rd</sup> February 2011. Locations of relatively high-

909 emissions, are observed in the Singapore Downtown Core area in the south-center of  
910 Singapore and in other locations throughout the island.

ACCEPTED MANUSCRIPT

**Highlights**

We present a novel method for predicting air pollution emissions using transport data

Study uses measured microscopic transport data and a microscopic emissions model

GPS data from over 15000 vehicles were analyzed to quantify speeds and accelerations

CO<sub>2</sub>, NO<sub>x</sub>, VOCs and PM were modeled in high spatio-temporal resolution

Highly localized areas of elevated emissions were identified